Study on the risk level of light pollution based on satellite remote sensing image data

Lanyu Jin[1,*], Yangyang Qin[2], Tianwei Ma[3]

[1]School of Materials Science and Engineering, Beijing Institute of Technology, Beijing, China, 100081

[2]School of Computer Science and Technology, Beijing Institute of Technology, Beijing, China, 100081

[3]School of Optoelectronics, Beijing Institute of Technology, Beijing, China, 100081

*Corresponding author: 2830956219jly@sina.com

Abstract. Light pollution caused by artificial lighting at night (ALAN) is attracting more and more attention. In order to develop a widely applicable light pollution risk level measurement standard and accurately assess the local light pollution risk level, this paper establishes a RIM model, proposes a light pollution risk score based on satellite remote sensing image data to measure the light pollution risk level in an arbitrary area, and visualizes the model solution results by Matlab. Specifically, this paper selects the "satellite remote sensing-environmental measurement" method to obtain the data, and adopts the double difference robust regression algorithm to reduce the influence of outliers on the model and improve the validity of the model. By iterating over a large amount of data, a cubic polynomial regression equation between the independent variable and illumination was determined. Finally, the established model was applied to measure the light pollution risk levels of four types of sites.

Keywords: light pollution risk leve, light pollution caused by artificial lighting at night, Robust regression algorithm, RIM Model.

1. Introduction

In recent years, light pollution has become an increasing influence and threat to the environment, affecting the stable ecological development to some extent. At present, the light pollution brought by human urban development mainly includes white bright pollution, artificial daylight pollution, and colored light pollution. Light pollution has a considerable negative impact on a wide variety of areas, including cities, suburbs, rural areas, and protected lands. Excessive artificial light at night affects the stability of ecosystems[1] as well as human physiological and psychological health, and the glare formed by artificial light may also lead to some motor vehicle accidents. Therefore, it is necessary to take appropriate measures to alleviate the negative effects brought by light pollution.

Of course, artificial light also has some positive effects, such as providing lighting for nighttime production and reducing community crime rates. The impact of different types of artificial light on ecosystems, human health, and production life varies from region to region.

In order to develop a widely applicable measure of light pollution risk level (RPRL) and accurately assess the local light pollution risk level, many scholars have done research.Walker model [2], although but has some predictive effect on the siting of observatories and on the analysis and control of urban light pollution, does not take into account the distribution of light sources, the number of light sources, wattage and the amount of reflected light in the calculation results. Although Cinzano P [3] considered the effect of the sum of light sources in a decentralized and continuous urban (town) area on light pollution in areas other than the light sources, their model is too complex and not easy to understand for generalization.

Therefore,we developed a widely used measure to assess the RPRL of an area. The developed RIM model was applied to score and interpret four different types of locations based on population density and accessibility to the city.

2. Remote-Sensing Illumination Measurement (RIM) Model

We first chose the "satellite remote sensing-environmental measurement" method to evaluate ALAN, and used the Bisquare robust algorithm to regress the radiance and illuminance values, and selected the cubic regression equation with the largest correction coefficient. As a result, we obtained the mapping relationship between illuminance and light pollution risk score, and developed a model to assess RPRL

2.1. Selection of Measurement Methods

Digital illuminance meters are generally used to measure the illuminance in the environment by deploying them to collect data at multiple observation points in neighborhoods, indoor, and community scenes [4]. However, the direct measurement method is not only expensive, time-consuming, and difficult to operate, but also difficult to apply to a large scale study of light pollution. However, direct measurement is not only costly, time-consuming, and difficult to apply to a large scale study of light pollution. In contrast, satellite remote sensing images are easier to obtain and cover a wider area, which can efficiently provide sufficient data for the study. By correlating the horizontal illuminance of the measurement point with the radiance values obtained from satellite remote sensing images, we found a strong positive correlation between the two. Finally, the RIM model was established by regression analysis of the horizontal direction illuminance and radiance values of measurement points, so that the environmental horizontal direction illuminance of the formulated area can be quickly obtained from satellite remote sensing images. The spatial resolution of DMSP/OLS and NPP/VIIRS is low (5km and 750m respectively) [5], which cannot provide sufficient spatial detail information. In contrast, the Luojia-1 (LJ-1) satellite can provide remote sensing images with 130m spatial resolution, which provides data with large coverage area and high accuracy for the study and detection of light pollution. The GM1040 digital illuminance meter produced by Benetech was used to measure the illuminance (Ev) in the environment according to the study by Li Jiayi et al. [6]. The satellite remote sensing image data used in this study is the data taken by the LJ1-01 satellite on the evening of November 23, 2018 (resolution 130m, Figure 1), from the official website of LJ-1 data [7]. The ground data were selected from the measurements of the GM1040 digital illuminance meter manufactured by Benetech.

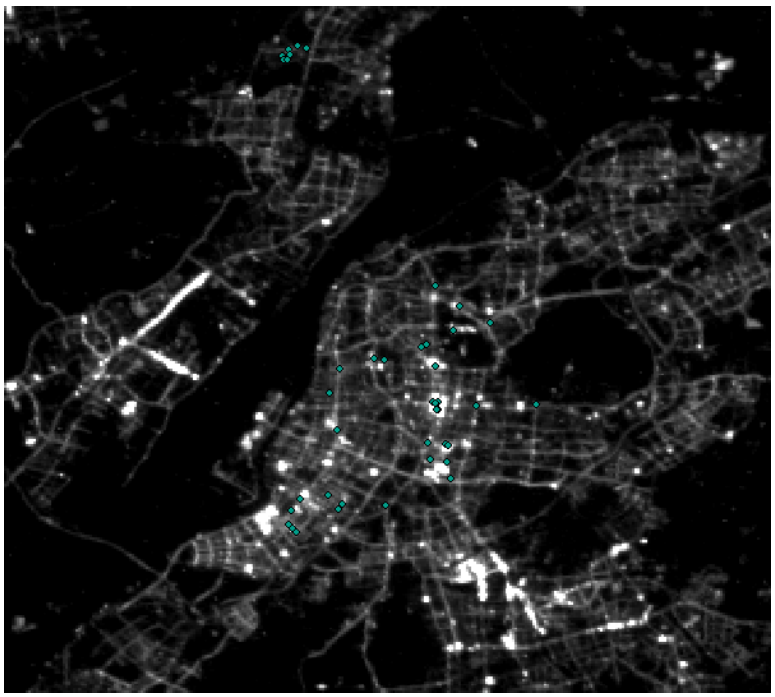


Figure 1. Remote sensing images and measurement points of Luojia-1 satellite (marked in green in the picture) [7]

2.2. The Establishment of RIM Model

Catherine Pérez Vega et al. compared the use of various physical quantities of light in the field of urban lighting planning and nighttime artificial lighting research, they found that the illuminance of ALAN is one of the physical quantities that researchers are most concerned about. At the same time, it is the main factor that causes and affects light pollution[8]. Therefore, we decide to ignore the influence of other physical quantities of light on light pollution and to measure the light pollution level of an area mainly by the illuminance of light in the nighttime environment. According to the International Commission on Illumination's publication "Guidelines for the Limitation of the Impact of Disturbing Light from Outdoor Lighting Facilities" [9], the relevant lighting technology indicator for the impact of disturbing light on residents is "window vertical illuminance". In most cases, this can be approximated as the horizontal illuminance in the environment. Meanwhile, Li Jiayi's research as well as actual data prove that there is a strong positive correlation between horizontal light and ambient light [6], where the correlation coefficient between horizontal illuminance and vertical illuminance is high at all measurement points (r=0.88092, Figure 2). Therefore, we believe that measuring the degree of light pollution in an area by the horizontal illuminance of light in the nighttime environment can better reflect the negative effects of artificial light in the horizontal and vertical directions on residents and other organisms at night.

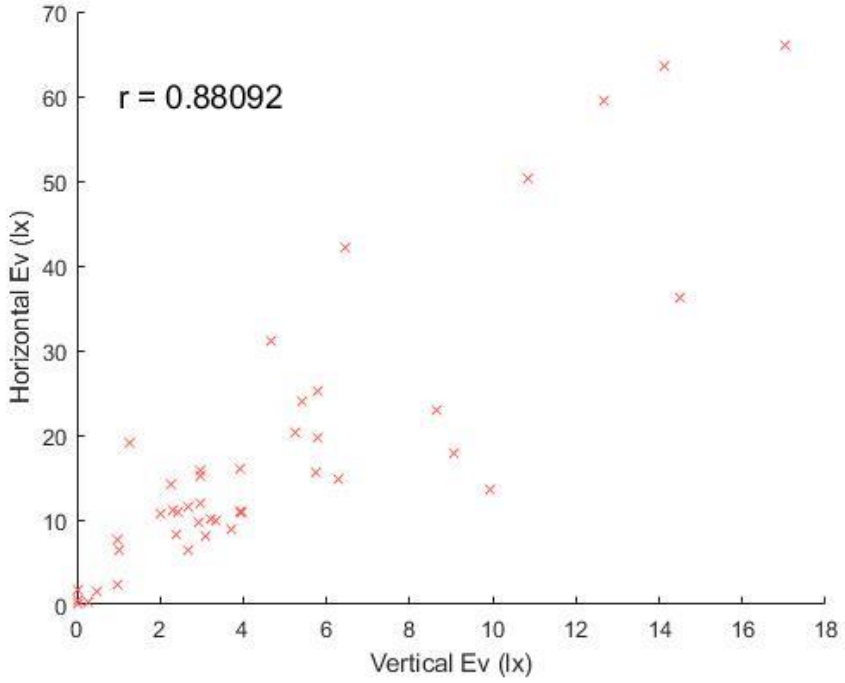


Figure 2. Scatter plot of horizontal illuminance and vertical illuminance [6]

According to the official correction equation of LJ-1, we obtained the corresponding radiance values from the grayscale values of the measured points in the remote sensing image:

$$G = DN^{1.5} \cdot 10^{-10} \tag{1}$$

Among the selected measurement points, the radiance values and horizontal illuminance show a strong correlation(r=0.72346, Figure 3).

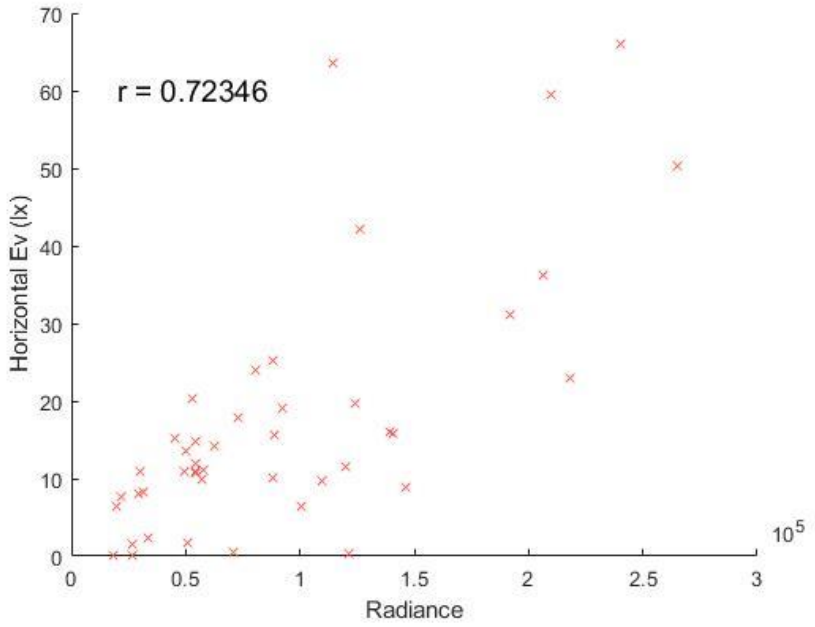


Figure 3. Scatter plot of radiance values versus horizontal illuminance

The five empirical models established are compared by considering the radiance value of LJ1-01 as the independent variable and the ambient illumination as the dependent variable, determining the algorithm for optimal estimation of the ambient illumination of LJ1-01 images. The specific equations are as follows:

Single linear model:

$$E_v = \alpha G + \beta \tag{2}$$

Quadratic polynomial model:

$$E_v = \alpha G^2 + \beta G + \gamma \tag{3}$$

Trigonometric polynomial model:

$$E_v = \alpha G^3 + \beta G^2 + \gamma G + \delta \tag{4}$$

Exponential model:

$$E_v = \alpha e^{\beta G} \tag{5}$$

Binomial Index model:

$$E_v = \alpha e^{\beta G} + \gamma e^{\delta G} \tag{6}$$

The E_v is the ambient E_v(lx), R is the radiance of the pixel (10^{-6}W·m^{-2}·sr^{-1}·μm^{-1}), and α, β, γ *and* δ are the regression coefficients.

Since the numerical order of magnitude difference between the radiance values and the horizontal illuminance is too large, we centered and scaled the radiance values to eliminate the effect of data units and to speed up the iterative solution of the regression coefficients.

$$G' = \frac{G-\mu}{\sigma} \tag{7}$$

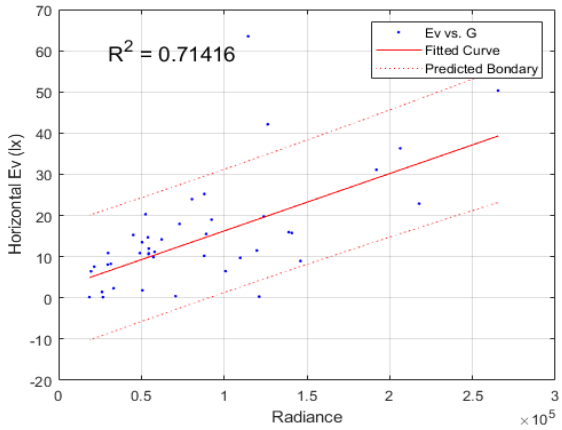
Where, μ、$\sigma$are the mean and standard deviation of the overall irradiance values, respectively.

We also used Bisquare (Bisquare) for robust analysis to remove the effect of some outliers.

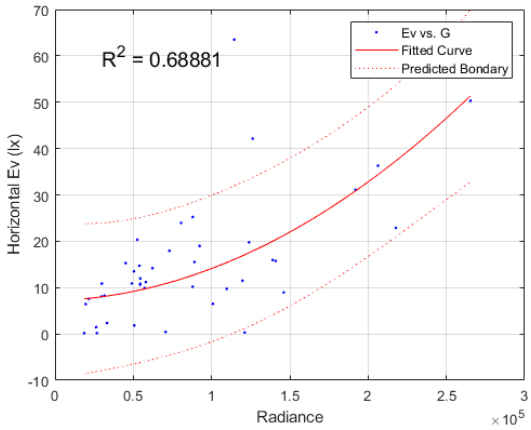
The root mean square error (RMSE) and the correction coefficient of determination (R^2) were calculated as performance metrics.

$$RMSE = \sqrt{\frac{\sum_{i=1}^{m}\left(E_{vi} - \widehat{E_{vi}}\right)^2}{m}} \tag{8}$$

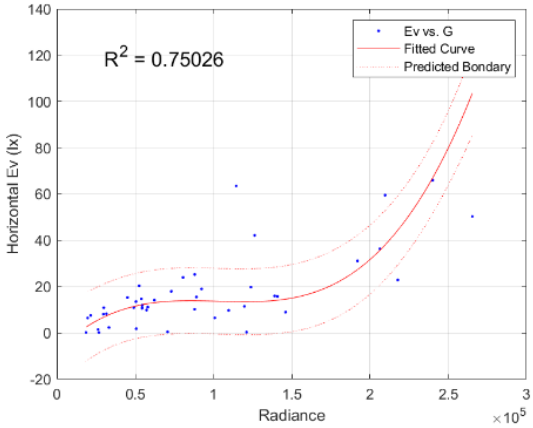
$$R^2 = 1 - \frac{\sum_{i=1}^{m}\left(E_{vi} - \widehat{E_{vi}}\right)^2}{\sum_{i=1}^{m}\left(\overline{E_v} - E_{vi}\right)^2} \tag{9}$$



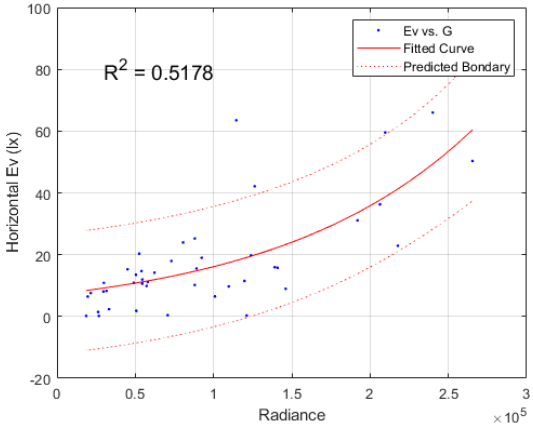
(a) Single linear model



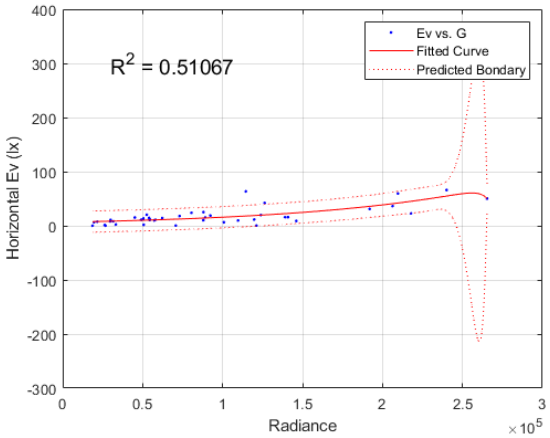
(b) Quadratic polynomial model



(c) Trigonometric polynomial model



(d) Exponential model



(e) Binomial Index model

Figure 4. Fitting results of the five models

After analyzing the results of the five model store fits (Figure 4), we finally decided to use the three-term model as the final fitting model. The complete fitting equation is as follows:

$$E_{\mathrm{v}} = \alpha(\frac{G-\mu}{\sigma})^3 + \beta(\frac{G-\mu}{\sigma})^2 + \gamma\frac{G-\mu}{\sigma} + \delta \tag{10}$$

Where, $\alpha = 5.602, \beta = -2.876, \gamma = -0.7668, \delta = 13.85, \mu = 91710, \sigma = 63780.$

2.3. Discussion of results

We specify the range of regional light pollution risk level coefficient between 0 and 100, and establish the mapping relationship between horizontal illuminance and light pollution risk level coefficients in the nighttime environment, and to set the regional light pollution risk level classification criteria.

$$R_l = \begin{cases} 4E_{\mathrm{v}}, & E_{\mathrm{v}} \leq 25 \\ 100, & E_{\mathrm{v}} > 25 \end{cases} \tag{11}$$

Based on the light pollution risk level scores obtained from the model, we classify the pollution level into the following four classes. Since areas with scores greater than 100 hardly occur in our calculations, the classification is shown in Table 1.

Table 1. Regional light pollution risk level grading standards

R_l ranking	0-25	26-50	51-75	76-100
Pollution level	Slight pollution	Mild pollution	Medium pollution	Heavy pollution

Based on the above model, we analyze the following four locations as representatives of different types of regions.

3. Case Studies of RIM Model

We selected one community in each of the four types of areas: urban, suburban, rural, and conservation areas for the study. After obtaining the grayscale values of the raster corresponding to the selected sites using arcGIS software, their RPRL scores and pollution levels were derived using the RIM model. Their RPRL were discussed in the context of the actual situation. It was verified that the RIM model passed the sensitivity test.

3.1. Information Description

Considering the influence of climatic zones on RPRL, we selected only four types of regions within Jiangsu Province, China, as experimental subjects in order to use region type as the only variable. (1) A protected land The Yangtze finless porpoise provincial nature reserve (118.74117°E, 32.09660°N) is located in Jiangsu province and covers a wide area. The current in this area is slow and there are few boats in the waterway. It has a variety of marine life and birds, rare finless porpoises, and complete safety lighting measures. This site is protected from development because of its importance to natural ecological development. (2) A rural community The Orchid Pond (118.55957°E, 31.95935°N) is a rural area in Jiangsu province with flat land and a relatively sparse population. The community is mainly characterized by poultry and livestock farming, especially lobster farming has become large-scale, which requires a certain degree of lighting measures. Due to the lack of advanced equipment, the light pollution caused by artificial light is neglected and the negative impact may be large. (3) A suburban community Gaoke Rongjing (118.98734°E, 32.12800°N) is a villa community in the suburbs of Jiangsu Province, characterized by more private courtyards and commercial clubs, etc., which may have large light sources due to non-interference. There are large public parking lots located underground, and private parking is available in the garage, which may bring more serious light pollution. (4) An urban community Hejiacun (118.83241°E, 32.10990°N) is a community

located in Jiangsu Province, within the eight districts of Nanjing's main city. It is a modern riverside area with a combination of science, technology, education and scenic beauty. This area has well-developed transportation, frequent human activities, and a high level of awareness of light pollution.

3.2. The Applications of RIM Model

After the latitude and longitude of the four typical locations are selected and determined, the grayscale values of the image elements at the four coordinates are derived by arcGIS software and then substituted into equation (1) to obtain the corresponding radiance values at the coordinates, followed by substituting the radiance values into equation (5) to obtain the fitted values of the RIM model for the illuminance of the four locations in the horizontal direction of ALAN. Then the fitted illuminance values are mapped by equation (6) to obtain the light pollution risk scores, and finally the scores are compared with the table 2 to assess the RPRL of the four selected locations.

3.3. Interpretation of Results

We visualize the measurement results in Figure 5:

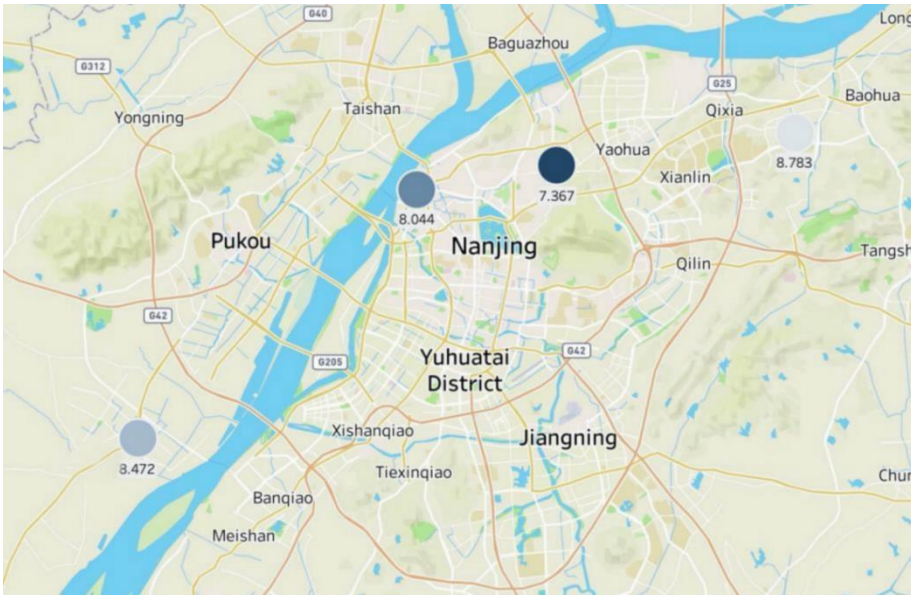


Figure 5. Light pollution level scores for four locations

The R_l ranking of the four locations were calculated as suburban (35.1) > rural (33.9) > protected area (32.2) > urban community (29.5). Three quarters of the sites are moderately polluted, and only the Hejiacun community is lightly polluted. This may be due to its high greening standard, strong awareness of light pollution prevention, and the high ecological requirements of downtown residents. The most serious light pollution is in the suburban area of Gaoke Rongjing district, which may be caused by the fact that the suburban area is less regulated and has not had strict regulations on light pollution prevention or intervention [10]. Although the porpoise in the reserve cannot be disturbed by more ALAN, the river will be properly illuminated for security reasons precisely because of the high conservation requirements in the area. Although the population density of Orchid Pond is low, its pollution level is moderately high. We presume that because Orchid Pond is one of the famous tourist attractions, more lighting is used in this area for the purpose of attracting tourists and showing the idyllic scenery.

3.4. Sensitivity Analysis

The sensitivity$S(R_l, DN)$ reflects the relationship between the relative change of DN and the relative change it causes in R_l , which is calculated as follows:

$$S(R_l, DN) = \frac{dR_l}{dDN} \cdot \frac{DN}{R_l} = \frac{dR_l}{dG} \cdot \frac{dG}{dDN} \cdot \frac{DN}{R_l} = \frac{16 \times 10^{-10} \cdot \left[3\alpha\left(\frac{G-\mu}{\sigma}\right)^2 + 2\beta\left(\frac{G-\mu}{\sigma}\right) + \gamma\right]}{DN^{0.5}\left[\alpha\left(\frac{G-\mu}{\sigma}\right)^3 + \beta\left(\frac{G-\mu}{\sigma}\right)^2 + \gamma 3\alpha\left(\frac{G-\mu}{\sigma}\right)^2 + 2\beta\left(\frac{G-\mu}{\sigma}\right) + \gamma\right]} \quad (12)$$

After adjusting the DN of each of the four selected locations up or down by 5%, the RIM model is used to derive the changed Ev (Figure below). When the DN is changed by 5%, the relative change in light pollution score is around 1.35%. The results obtained from the above method are as follows:

4. Conclusions

Today, light pollution caused by artificial lighting at night (ALAN) is raising more and more concerns. We need to set widely applicable measurement standards for light pollution risk level (RPRL) and develop lighting control strategies for different locations.

This paper selected the "satellite remote sensing-environmental measurement" method. The data were obtained for fitting. The data were centered and scaled to eliminate the effect of dimensionality and to improve the convergence speed of the model iteration. And the Bisquare robust regression algorithm was used to reduce the effect of outlying points on the model and improve the validity of the model. After iterating over a large amount of data, a cubic polynomial regression equation between the independent variable and the dependent variable was determined. We established the RIM model to propose the light pollution risk score based on satellite remote sensing image data to measure the RPRL of any region, and the model solution results were visualized by Matlab.

Applying the RIM Model, we measured RPRL for four types of sites and found that urban RPRL is significantly lower than both suburban and rural areas, which is consistent with common sense. However, there is no clear pattern of RPRL in protected locations, and it depends on site-specific analysis.

References

[1] Hölker F, Bolliger J, Davies T W, et al. Pressing research questions on how light pollution affects biodiversity[J]. Front. Ecol. Evol. 9, 767177. 2021.

[2] Cinzano P, Disentangling artificial sky brightness from single sources in diffusely urbanized areas, Journal of the italian astronomical society, 2000,71(1): 113-131.

[3] Cinzano P, The Propagation of Light Pollution in Diffusely Urbanised Areas, Memorie della Societa Astronomia Italiana, 2000, 71(1):93~112.

[4] Tong J C K, Lau E S L, Hui M C Y, et al. Light pollution spatial impact assessment in Hong Kong: Measurement and numerical modelling on commercial lights at street level[J]. Science of The Total Environment, 2022, 837: 155681.

[5] Chen X, Liu HH, Li JH, et al. Analysis of coupled urbanization and ecological environment coordination based on nocturnal remote sensing[J]. Remote Sensing of Natural Resources,2022,34(04):280-285.

[6] Li Jiayi, Xu Yongming, Cui Weiping et al. Nighttime light pollution monitoring in Nanjing based on Liaojia-1 nighttime remote sensing data[J]. Remote Sensing of Natural Resources,2022,34(02):289-295.

[7] http://59.175.109.173:8888.

[8] Pérez Vega C, Zielinska-Dabkowska K M, Schroer S, et al. A systematic review for establishing relevant environmental parameters for urban lighting: Translating research into practice[J]. Sustainability, 2022, 14(3): 1107.

[9] Li Yuan,Li Tienan.Explanation of changes in the revision of CIE 150 "Guidelines for the limitation of disturbing light impacts from outdoor lighting facilities"[J]. Journal of Lighting Engineering,2018,29(06):40-45.

[10] Xu Huimin,Hu Shougeng. Spatial and temporal evolution of urban scale in China from the perspective of luminous remote sensing[J]. Journal of Wuhan University (Information Science Edition),2021,46(01):40-49.DOI:10.13203/j.whugis20190330.